

Original Article

Speciation and hybridization of *Enkianthus quinqueflorus* and *E. serrulatus* (Ericaceae) across a tropical–subtropical transitional zone in South China

Wan Hu^{1,2, ID}, Qi Qiu¹, Hua Liang¹, Yang Liu¹, Yi Yang^{1,4}, Yixuan Kou^{3,5}, Shudong Zhang⁶, Dengmei Fan^{1,4,*}, Zhiyong Zhang^{1,3,5,*}

¹Laboratory of Subtropical Biodiversity, College of Forestry, Jiangxi Agricultural University, Nanchang 330045, China

²Lushan Botanical Garden, Jiangxi Province and Chinese Academy of Sciences, Jiujiang 332900, China

³Key Laboratory of Ecology of Rare and Endangered Species and Environmental Protection (Guangxi Normal University), Ministry of Education, Guilin 541004, China

⁴Jiangxi Provincial Key Laboratory of Conservation Biology, College of Forestry, Jiangxi Agricultural University, Nanchang 330045, China

⁵University Engineering Research Center of Bioinformation and Genetic Improvement of Specialty Crops, Guangxi, Guilin 541006, China

⁶School of Biological Science and Technology, Liupanshui Normal University, Liupanshui 553004, China

*Corresponding author. Key Laboratory of Ecology of Rare and Endangered Species and Environmental Protection (Guangxi Normal University), Ministry of Education, Guilin 541004, China. E-mail: pinus-rubus@163.com or zhangzy@gxnu.edu.cn; Laboratory of Subtropical Biodiversity, College of Forestry, Jiangxi Agricultural University, Nanchang 330045, China. dmf.625@163.com

ABSTRACT

How speciation and hybridization occur across steep environmental gradients has fascinated ecologists and evolutionary biologists for decades. *Enkianthus quinqueflorus* and *E. serrulatus* are a species pair located on the two sides of the Nanling Mountains, a previously proposed tropical–subtropical transitional zone (ecotone) of south China. In this study, we investigated its speciation and hybridization history based on DNA sequences of four chloroplast inter-genic spacers and eight nuclear genes from 44 populations. Phylogenetic analyses found clear cytonuclear discordance, indicating some *E. quinqueflorus* (EquiN) populations were of hybrid origin, largely corresponding to *E. serotinus* (especially *E. tubulatus*). Approximate Bayesian computation (ABC) analysis found that EquiN were derived from hybridization between *E. serrulatus* and the other cluster of *E. quinqueflorus* (EquiS) at 0.22 Mya after an initial split at 0.93 Mya, and the hybridization was also confirmed by IMa2. Ecological niche modelling indicated that *E. serrulatus* and EquiS had distinct ecological niches but with overlapped distribution across the late Quaternary. These results, coupled with morphological intermediacy of *E. tubulatus*, clearly suggest that *E. quinqueflorus* (EquiS) and *E. serrulatus* may be the products of allopatric speciation associated with refugial isolation during the late Cenozoic climate changes, and *E. tubulatus* could have resulted from second contact and hybridization around the Nanling Mountains between *E. quinqueflorus* (EquiS) and *E. serrulatus*. This study suggests that the Nanling Mountains are a hotspot of speciation and hybridization for woody flowering plants, and represent the tropical–subtropical transitional zone in south China, at least in terms of plant divergence and speciation.

Keywords: allopatric speciation; biogeographical boundary; ecotone; *Enkianthus*; hybrid zone; hybridization; Nanling Mountains

INTRODUCTION

The process by which individuals from genetically distinct populations (e.g. species, subspecies) mate and produce at least some viable offspring is referred to as hybridization, and the geographically narrow areas where hybridization is localized are hybrid zones (Barton and Hewitt 1985, Harrison 1993, Gompert *et al.* 2017). Hybrid zones can show complex patterns in space. In many cases, hybrid zones tend to be located at ecotones

between habitats occupied by parental forms (Barton and Gale 1993, Moore and Price 1993), as ecotones always coincide with areas of steep transition along environmental gradients or zones of threshold or nonlinear responses to gradual gradients in the physical environment (Risser 1995, Kark 2007, 2012).

Hybrid zones are ideal arenas to observe interactions between divergent gene pools and the study of hybrid zones at ecotones has played an important role in understanding the origin of

species (Barton and Hewitt 1985, Hewitt 1988, Abbott 2017, Stankowski *et al.* 2021, Wielstra 2021). Originally, some studies suggested that natural selection posed by steep environmental gradients at ecotones is the principal cause for the origin of species (e.g. Smith *et al.* 1997, Schneider *et al.* 1999, Schilthuizen 2000, Nosil 2012). Under such scenarios, primary hybrid zones can be formed between populations diverged in parapatry by differential environmental selection (Abbott 2017, Stankowski *et al.* 2021, Wielstra 2021). By contrast, reproductive isolation is considered more commonly a by-product of genetic drift and local adaptation in allopatry (Mayr 1959, Coyne and Orr 2004), and most hybrid zones across ecotones seem to originate by secondary contact between populations that diverged in allopatry (Abbott 2017). Moreover, distinct habitats always exist at ecotones between the two adjoining habitat types (Kark 2007, 2012), where hybrids with intermediate phenotypes may be best fitted, giving rise to stable hybrid superiority zones (bounded superiority zones) (Abbott 2017, Stankowski *et al.* 2021). Sometimes, those hybrid individuals may have 'transgressive' phenotypes that outperform either parental type (Rieseberg *et al.* 1999), or become isolated from their parents due to changes in distribution ranges (e.g. Wang and Szmidt 1990, DeRaad *et al.* 2023), leaving behind a new hybrid species.

Latitudinal gradients in abiotic factors, especially temperature gradients, strongly determine species distribution and genetic divergence (Pereira *et al.* 2017). Freezing temperature can cause lethal injuries in living plant tissues (Sakai and Larcher 1987) and have long been considered a principal restriction on the spreading out of the tropics for many tropical plant lineages (Donoghue 2008). At the northern/southern limit of the tropical zone, there is a sharp decrease in tropical seed plant elements because they cannot withstand freezing temperature (Donoghue 2008, Cavender-Bares *et al.* 2011, Fan *et al.* 2022), resulting in a transitional zone from tropical zone to subtropical (warm-temperate) zone. Because such transitional zones have occasionally been referred to as 'ecotones' in previous literature (Ashton and Zhu 2020), we use 'transitional zone' and 'ecotone' interchangeably in this study. In the tropical–subtropical transitional zone of south and south-west China, high plant species richness has been reported for flower plants as a whole (Ye *et al.* 2019a) or a particular plant group (e.g. Lauraceae, Zhou *et al.* 2023), possibly due to different species from the adjoining tropical and subtropical zones meeting at the ecotone. More importantly, accumulating evidence indicates that this ecotone might be a hotspot of population divergence, speciation, and hybridization, possibly due to the nonlinear physiological responses to temperature gradient around freezing point and range shift caused by glacial-interglacial climate changes during the late Cenozoic (Ye *et al.* 2019a, Chen *et al.* 2022, Fan *et al.* 2022). Therefore, this ecotone represents an active area of speciation and hybridization, deserving more attention from ecologists and evolutionary biologists.

In south and south-west China, however, several northern boundaries of the tropical zone have been recommended based on various criteria. For example, Zhu and his colleagues (Zhu 2013, Ashton and Zhu 2020) recommended a line at roughly 22° 30' N, but Zhu and Wan (1963) proposed a line along the Nanling Mountains (roughly the line at 24° N–25° N). However, these lines are delineated according to qualitative evidence

such as phenological observations (Zhu and Wan 1963) or plant distribution patterns (Zhu 2013, Ashton and Zhu 2020), mostly lacking a quantitative operational criterion. By combining geographically explicit information and population genetic data, phylogeographic structure within species or among closely related species has become a powerful tool for biogeographical regionalization (e.g. Lin *et al.* 2018, Rana *et al.* 2023). Several phylogeographic studies have revealed that there is an ecophysiological boundary along the Nanling Mountains (Fan *et al.* 2016, 2022, Ye *et al.* 2019b), indicating a line along the Nanling Mountains might represent the tropical–subtropical transitional zones in south China, at least in terms of plant population divergence and speciation. However, such studies are still scarce and more empirical cases should be documented to verify this finding.

Enkianthus Lour. (Ericaceae) is a genus of shrubs or small trees occurring in E. Himalayas, south China (including Taiwan), Japan, and Indochina (Fang and Stevens 2005). Anderberg (1993) recommended four sections within the genus: *Enkiantella*, *Meisteria*, *Andromedina*, and *Enkianthus*. Sect. *Enkianthus* distributed in central to south China and Japan, is a monophyletic clade according to previous molecular phylogenies (Tsutsumi and Hirayama 2012, Liang *et al.* 2022). Within sect. *Enkianthus*, there are two sister diploid species, *Enkianthus quinqueflorus* Lour. and *E. serrulatus* (Wils.) Schneid. (Liang *et al.* 2022), then together sister to *E. perulatus* C. K. Schneid. *Enkianthus quinqueflorus* is roughly located to the south of the Nanling Mountains, while *E. serrulatus* to the north (Fig. 1A). Besides the three species, there is another formally recognized species (*E. serotinus* Chun et Fang) within the sect. *Enkianthus* (Fang and Stevens 2005). Although this species has been recorded sporadically in Guangdong, Guangxi, Guizhou, Sichuan, and Yunnan (Fang and Stevens 2005), our extensive field investigations found that this species is confined mainly to the Nanling Mountains (Fig. 1A). Intriguingly, the morphology of *E. serotinus* is intermediate to *E. quinqueflorus* and *E. serrulatus*, possessing leathery leaves like *E. quinqueflorus*, but white flowers like *E. serrulatus*, implying that *E. serotinus* might be derived from hybridization between *E. quinqueflorus* and *E. serrulatus* and the Nanling Mountains might be a hybrid zone between the two. In addition, the two adjoining species have distinct life habits (*E. quinqueflorus* is evergreen with leathery leaves but *E. serrulatus* is deciduous with papery leaves), alluding that the two species might be the products of parapatric speciation (a form of ecological speciation with gene flow, Nosil 2012) under ecological pressure associated with freezing temperature at the tropical–subtropical ecotone (Zanne *et al.* 2014) and the hybrid zone between them might be of primary intergradation. However, range shifts and refugial isolation during the Quaternary climate changes have been considered the causative factor in population divergence and speciation across the tropical–subtropical ecotone (Chen *et al.* 2022, Fan *et al.* 2022, Ye *et al.* 2019b), allopatric speciation, and secondary contact might be more plausible for *E. quinqueflorus* and *E. serrulatus*. Therefore, unveiling the speciation and hybridization history of *E. quinqueflorus* and *E. serrulatus* is crucial for understanding the formation of the hybrid zone at the tropical–subtropical ecotone and the phylogeographic structure among the two species would be constructive for determining the position of the tropical–subtropical ecotone.

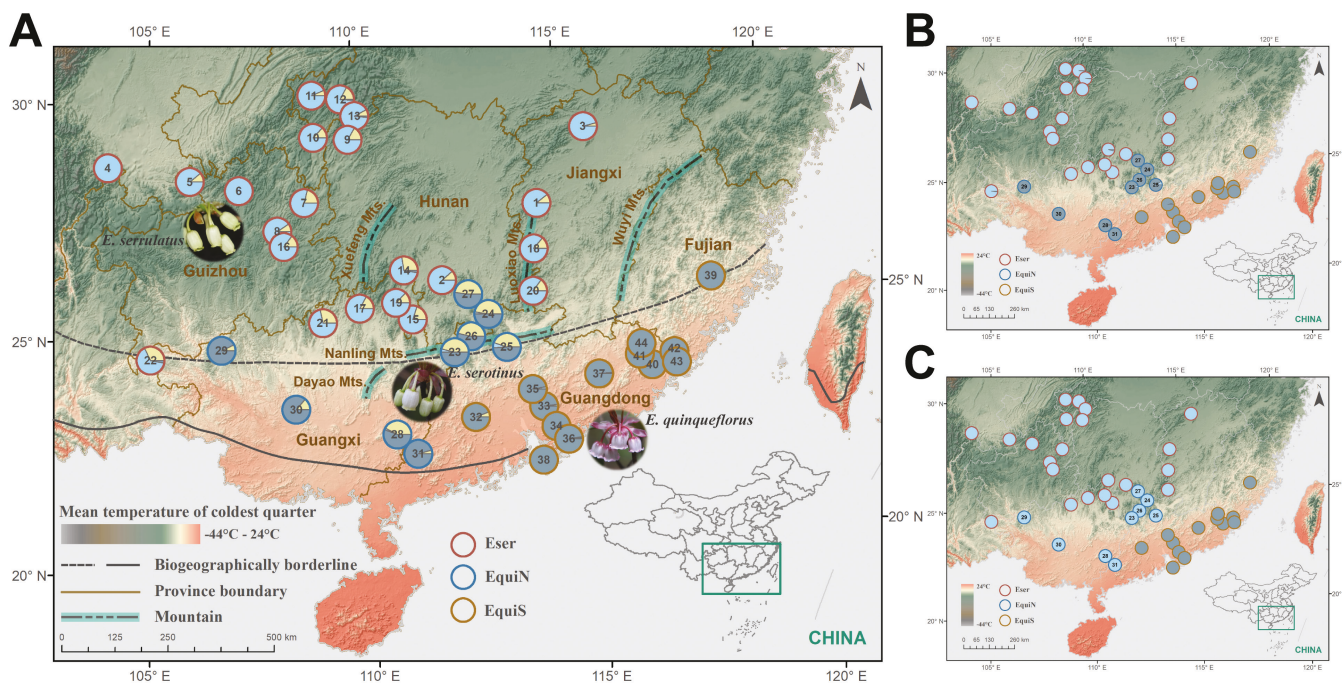


Figure 1. Geographic distribution of genetic clusters. A, Pie charts show the mixed ancestry when $K = 3$ inferred by STRUCTURE. Three distinct genetic groups are identified by their coloured circles. The inset images show the typical flower morphology of the three *Enkianthus* species distributed in the corresponding geographical region, as recorded in *Floral of China*. The figure illustrates the two biogeographically northern boundaries of the tropical area in south and southeastern China, respectively, a solid line at $22^{\circ}30'N$ recommended by Zhu (2013), and a dotted line along the south of Nanling Mountains (roughly the line at $24^{\circ}N$ – $25^{\circ}N$) proposed by Zhu and Wan (1963). The background colours show the mean temperature of coldest quarter. B, C, The ancestry composition of each population for $K = 2$ is shown in geography based on the nuclear gene data set (B) and chloroplast DNA (C).

Here, we collected population samples across the ranges of *E. quinqueflorus* and *E. serrulatus* as well as the putative hybrid species, *E. serotinus*. Four chloroplast regions and eight nuclear genes were screened and sequenced. By integrating approaches of population genetics, molecular phylogenetics and ecological niche modelling, we address the following: (i) whether *E. quinqueflorus* and *E. serrulatus* resulted from parapatric speciation or allopatric speciation. (ii) Whether *E. serotinus* is derived from hybridization between *E. quinqueflorus* and *E. serrulatus* and whether there is a hybrid zone between them. (iii) Do the Nanling Mountains represent the tropical–subtropical transitional zone from the perspective of plant divergence and speciation?

MATERIALS AND METHODS

Sampling and DNA extraction

Leaf samples were obtained from 22 populations ($n = 122$) of *E. serrulatus* and 22 populations ($n = 121$) of *E. quinqueflorus* throughout their ranges in China (Table S1 in the Supporting Information). The latter included the putative hybrid species *E. serotinus* because it is difficult to distinguish *E. serotinus* from *E. quinqueflorus* practically due to both having leathery leaves and occasionally *E. quinqueflorus* bearing white flowers like *E. serotinus*. To avoid arbitrary taxonomic identification, we treated the putative *E. serotinus* populations as *E. quinqueflorus* temporarily. Fresh leaves were dried in silica gel immediately after collection, and all sampled individuals from each

population were spaced at least 10 m apart. Voucher specimens were deposited in the Herbarium of Lushan Botanical Garden of the Chinese Academy of Sciences (LBG). Total genomic DNA was extracted from desiccated leaves using a modified cetyltrimethylammonium bromide (CTAB) procedure (Doyle and Doyle 1990).

Meanwhile, to delineate the species relationships based on morphology, we quantified seven floral traits (florescence number, corolla diameter, corolla length, pedicel length, stamen length, stigma height, and the difference in length between the stamen and stigma) in five populations (20, 23, 24, 36, and 38), each comprising a minimum of 10 individuals. Three replicates of each individual were randomly selected for trait measurement. Principal component analysis (PCA) was then performed on the measured trait datasets.

Locus screening, PCR amplification, and sequencing

Four intergenic spacer regions of chloroplast (cp) DNA (*petA-psbJ*, *rpl32-trnL*, *trnL-F*, *psbA-trnH*) were selected, amplified, and sequenced. In addition, eight single/low-copy nuclear genes (En23, En28, En61, En64, En72, En78, En80, and En93) were developed from transcriptome sequences of *E. serrulatus* following the method described in our previous studies (Kou *et al.* 2020, Fan *et al.* 2022). Transcriptome sequencing was performed on the Illumina NextSeq 500 platform (Illumina, San Diego, CA, USA) at Personal Biotechnology (Shanghai, China). The sequences of transcriptome unigenes were deposited in figshare (<https://doi.org/10.6084/m9.figshare.23815533>). Protocols of

PCR amplification and DNA sequencing followed by *Fan et al.* (2022), with different annealing temperature settings for each locus (Table S2 in the Supporting Information).

Raw chromatograms were checked and edited using Sequencher v.5.4.6 (GeneCodes Corporation, Ann Arbor, MI, USA), aligned using BioEdit v.7.2 (Hall 1999), and then refined manually in MEGA v.7.0 (Kumar *et al.* 2016). The nuclear sequences were phased in DnaSP v.5.1 (Librado and Rozas 2009) for performing downstream analyses. All sequences have been deposited in GenBank under accession numbers OR382010–OR386929.

Genetic diversity, population differentiation, and neutrality test

For both cpDNA and nuclear loci, population genetic parameters were estimated using DnaSP v.5.1. For the concatenated cpDNA, the number of haplotypes (N_h), haplotype diversity (H_d), and nucleotide diversity (π) were calculated. For each nuclear locus, we estimated the number of segregating sites (S), nucleotide diversity (π), Watterson's parameter (θ_w) (Watterson 1975), the number of haplotypes (N_h), haplotype diversity (H_d), and the minimum number of recombinant events (R_m) after phasing sequences using the PHASE algorithm in DnaSP v.5.1. The expectation of neutral evolution was inferred for each locus using Tajima's D , Fu and Li's D^* and F^* (Fu and Li 1993).

Population differentiation based on ordered (N_{st}) and unordered (G_{st}) cpDNA haplotypes were calculated and then compared using U -statistics to test for the presence of phylogeographic structure. Genetic differentiation across eight nuclear loci within species as well as among populations within each species was computed using F_{st} (Wright 1951), and its significance (at each locus, and overall) was tested based on 1000 bootstrap permutations. All these analyses were performed using analysis of molecular variance in Arlequin v.3.0 (Excoffier *et al.* 2007).

Detection of hybridization

The existence of cytonuclear discordance was examined to detect whether a hybridization event happened between *E. quinqueflorus* and *E. serrulatus*. We inferred the maximum likelihood (ML) trees of all individuals using FastTree (Price *et al.* 2009) under the generalized time-reversible model with *E. chinensis* Franch. as outgroup based on eight concatenated nuclear genes as in *Zou et al.* (2013) and the concatenated cpDNA separately. The bootstrap support was calculated with 1000 replicates. We also constructed the genealogical relationships of haplotypes for each nuclear locus and the concatenated cpDNA using a median-joining network implemented in PopART v.1.7 (Leigh and Bryant 2015).

To further investigate the occurrence of hybridization, population structure was assessed by STRUCTURE v.2.3.4 (Hubisz *et al.* 2009) with the admixture model using single nucleotide polymorphisms of eight nuclear loci. Twenty independent runs were conducted for each number of clusters (K) ranging from 1 to 10 with a burn-in setting to 20 000 followed by 200 000 Markov chain Monte Carlo (MCMC) iterations. The LnP (D) (Pritchard *et al.* 2000) and ΔK statistic (Evanno *et al.* 2005) were used to estimate the most likely number of clusters.

Graphics were visualized using STRUCTURE Harvester (Earl and vonHoldt 2012). In addition, we analysed the genetic structure using PCA implemented in the R package 'pcaMethods' (Stacklies *et al.* 2007).

Inference of speciation, hybridization, and demographic history

We used the isolation with migration (IM) model to infer divergence time and gene flow of *E. quinqueflorus* and *E. serrulatus*. The model assumed neutrality, no selection, no recombination within loci, and random mating in ancestral and descendant populations (Hey and Nielsen 2004, 2007). We simulated and estimated the divergence time (t) and the bidirectional migration rate (m) between *E. quinqueflorus* and *E. serrulatus*, and effective population size (θ) using MCMC implemented in the IMa2 software package (Hey 2010). The simulations ran with a burn-in of 5 000 000 steps and retained 2 000 000 steps under the HKY mutation model. We set the mutation rate to 1.58×10^{-9} per site per year, which is estimated in *Rhododendron weyrichii* Maxim (Yoichi *et al.* 2016) in Ericaceae. We inferred the average generation time to 5 years according to our and Geng's (2000) observations.

Hybridization and divergence history of the two species were further evaluated using an ABC approach implemented in DIYABC v.2.1.0 (Cornuet *et al.* 2014). Three possible demographic scenarios were formulated based on the results of nuclear data. *E. quinqueflorus* (Equi) and *E. serrulatus* (Eser) split from an ancestral population at the time t_0 , then (1) *E. quinqueflorus* split into two clades (EquiN and EquiS) at the time t_1 ; (2) EquiN diverged from Eser at t_1 ; (3) EquiN was generated by a hybridization event between EquiS and Eser at t_1 (Fig. S1 in the Supporting Information). DIYABC selects the optimized rate from a given mutation range between 10^{-7} and 10^{-9} . Then 1 000 000 simulated datasets were generated for each scenario by default. Prior-scenario combinations were evaluated by performing a PCA on the summary statistics and comparing the overlap of the simulated and observed data. The posterior probabilities and 95% confidence intervals of our three scenarios were compared by weighted multigroup logistic regression on 1% of simulated datasets closest to the observed data, as implemented in DIYABC. The posterior distributions of coalescent parameters were estimated from the subset using a local linear regression procedure.

The temporal changes of effective population size were performed for each cluster independently with extended Bayesian skyline plots (EBSP) analysis in BEAST v.2.5 (Heled and Drummond 2008). We used the same substitution rate as in IMa2. The software jModel test v.2.1.7 (Darriba *et al.* 2012) was employed to choose the most suitable model during the creation of the input file through the BEAUTi package manager in BEAST. We set the MCMC to 10 000 000 steps with sampling every 10 000 steps and set the burn-in at 10%. Tracer v.1.7 was used to explore distribution convergence (Rambaut *et al.* 2018).

Ecological niche modelling and niche differentiation

To predict potential distributions of each species under the past and present climate envelopes, ecological niche modelling was carried out in MAXENT v.3.4.3 (Phillips and Dudík 2008) with

the settings as follows: replicates = 20; type = subsample; maximum iterations = 5000; random test points = 25%. Sampled records from 71 localities for *E. quinqueflorus* (excluding populations of EuiN) and 122 for *E. serrulatus* were obtained from field investigations and records retrieved from the Chinese Virtual Herbarium (<https://www.cvh.ac.cn/>). Nineteen bioclimatic variables with a 2.5 arc minute resolution were downloaded from the WorldClim database (<http://www.worldclim.org>) for each period: present day (1970–2000), the Mid-Holocene (MH, ~6000 years before present), the Last Glacial Maximum (LGM, ~22 000, MIROC model), and the Last Interglacial (LIG, ~120 000–140 000). The pairwise Pearson correlations (r) among the bioclimatic variables were examined to avoid multicollinearity, and we excluded one of the variables in each pair with $r > 0.7$. Eight bioclimatic variables (Bio2, mean diurnal range; Bio3, Isothermality; Bio8, mean temperature of wettest quarter; Bio10, mean temperature of warmest quarter; Bio11, mean temperature of coldest quarter; Bio15, precipitation seasonality; Bio16, precipitation of wettest quarter; Bio19, precipitation of coldest quarter) were retained. The AUC (area under the receiver operating characteristic curve) values were used to measure model accuracy and the model with values > 0.9 was considered better discrimination. We also conducted the Jackknife tests to identify the contribution of each climatic variable. The niche differences between the two species were measured by niche overlap and identity tests in ENMtools v.1.4.4 using statistics of Schoener's D and the standardized Hellinger distance (I) (Warren *et al.* 2008, 2010), which both range from 0 (no overlap) to 1 (complete overlap).

To further detect which climatic variable is associated with the genetic differentiation between the two species, and whether the boundary between genetic clusters corresponds to a transition between climatically distinct regions, we conducted a PCA on climate data (19 climate variables) located within the sampling sites. In addition, we evaluated the difference of each environmental variable between populations of two species using a nonparametric Kruskal–Wallis multiple-range test. The distribution of each environmental variable was displayed in kernel density plots. We performed these analyses and drew graphical illustrations in R v.3.6.3 (<http://www.R-project.org>).

RESULTS

Genetic diversity, genetic differentiation, and neutrality test

Four cpDNA-IGS regions were sequenced and aligned across 243 individuals of 44 *Enkianthus* populations with a total length of 3499 bp. The total haplotype diversity (H_d), overall gene diversity (H_T), and expected within-population gene diversity (H_s) of *E. serrulatus* (0.946, 0.977, and 0.350, respectively) were slightly higher than those of *E. quinqueflorus* (0.924, 0.956, and 0.220, respectively; Table S3 in the Supporting Information). Within the two clusters of *E. quinqueflorus* (see phylogenetic and STRUCTURE results next), EquiN was lower than EquiS for the three parameters (see details in Table S3 in the Supporting Information). However, the nucleotide diversity of *E. quinqueflorus* ($\pi = 0.00312$) was much higher than that of *E. serrulatus* (0.00130), while EquiN remained lower than EquiS. The phylogeographic structure was found in *E. serrulatus*,

E. quinqueflorus as a whole, and EquiS (N_{st} significantly larger than G_{st}), but not in EquiN.

For nuclear sequences, a total of 2760 bp were sequenced at eight nuclear loci (Table S4 in the Supporting Information). *Enkianthus quinqueflorus* exhibited overall higher genetic diversity, except for the average nucleotide diversity at nonsynonymous sites ($\pi = 0.00722$ in *E. quinqueflorus* versus $\pi = 0.00786$ in *E. serrulatus*). EquiS had higher average values for all parameters than EquiN, which is consistent with the cpDNA results. Significantly high population differentiation was observed in each nuclear loci for each pair of groups, with the average F_{st} for EquiS and EquiN (0.16428) exhibiting a lower value than that observed for the other pair of groups (Table S5 in the Supporting Information).

Negative values of Tajima's D and Fu and Li's D^* and F^* were estimated at all eight nuclear loci in both species (Table S6 in the Supporting Information). Most of these values were not significant in *E. serrulatus*, but significant in *E. quinqueflorus*, suggesting deviation from neutrality or demographic expansion.

Evidence of hybridization between *E. quinqueflorus* and *E. serrulatus*

The ML tree constructed from concatenated nuclear sequences identified two distinct clades, one corresponding to *E. serrulatus* (Eser), the other to *E. quinqueflorus* (except for one individual in population 23 (RY04) that is marked with an asterisk, Fig. 2A). On the cpDNA ML tree, however, the individuals of nine *E. quinqueflorus* populations (populations 23–31) clustered with *E. serrulatus* (coloured in yellow in Fig. 2B, C), displaying obvious cytonuclear discordance. Because these populations are located in the north of the *E. quinqueflorus* range, we then refer to them as EquiN, and other populations of *E. quinqueflorus* as EquiS (Fig. 2A, B). The results of median-joining networks of individual nuclear locus and cpDNA also showed obvious cytonuclear discordance (Fig. S2 in the Supporting Information).

In contrast to the results of phylogenetic analyses, STRUCTURE analysis indicated that only a few individuals of *E. quinqueflorus* showed mixed ancestry when $K = 2$ (Fig. 2B, C), which was optimally judged by $\text{Ln}P(D)$ and ΔK statistic (Fig. S3 in the Supporting Information). We further explored whether there was a substructure within each cluster when $K = 3$ and $K = 4$. For $K = 3$, the nine populations of *E. quinqueflorus*, especially populations 23–28, which show cytonuclear discordance in phylogenetic analyses displayed their own ancestry (coloured in yellow) (Figs 1A, 2C). Note that many populations of *E. serrulatus* also contained the yellow component to some extent, which might be caused by the sharing of ancestral polymorphisms as indicated in median-joining networks of individual nuclear locus (Fig. S4 in the Supporting Information). For $K = 4$, no meaningful substructure was detected. In the result of PCA, the first and second principal components (PCs) explained 40.06% and 13.81% of the total genetic variance. The first PC separated *E. quinqueflorus* and *E. serrulatus* and the second separated EquiN and EquiS with some mixture (Fig. 2D).

The PCA result of seven floral traits was consistent with the STRUCTURE result, with the three clusters exhibiting relatively distinct characteristics in 3D principal component space. The

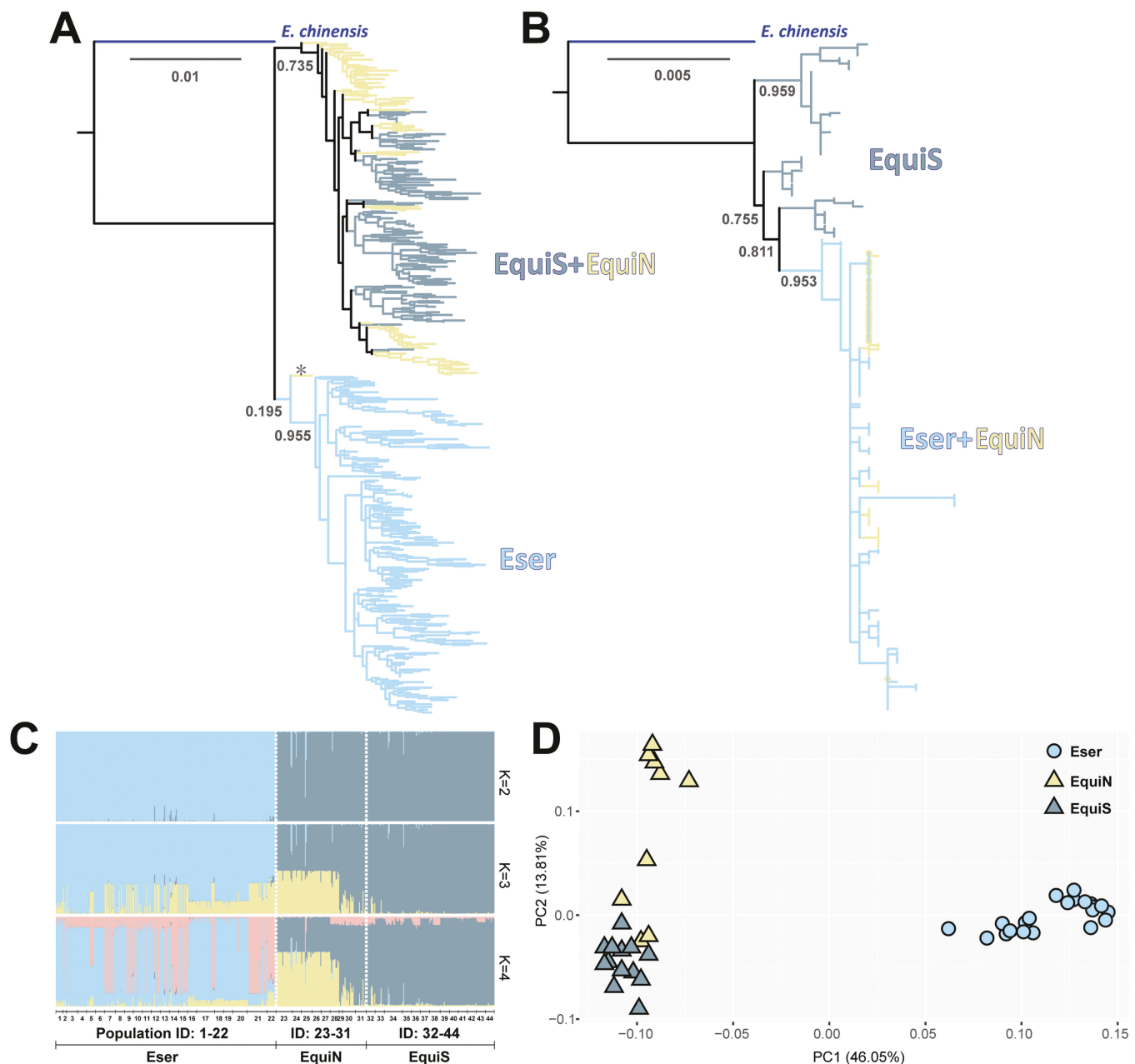


Figure 2. Phylogenetic relationships and population structure of the three genetic groups (Eser, EquiN, and EquiS). A, An ML tree based on eight nuclear loci that identified two distinct clades for *E. serrulatus* (Eser) and *E. quinqueflorus* (EquiN + EquiS), except RY04 (population 23) from EquiN, which is clustered with Eser and marked with an asterisk in the figure. B, An ML tree based on chloroplast DNA, among which the relationship between the EquiN and Eser group is the closest. The supporting values from bootstrap analyses are labelled main beside the nodes. C, Genetic structure with combined nuclear data for each individual of the three groups. The scenarios of $K = 2$, $K = 3$, and $K = 4$ are shown, and $K = 2$ is the best value according to cross-validation analysis. D, PCA on pairwise genetic differentiation of populations for three genetic groups based on eight nuclear loci.

floral morphology of EquiN was approximately intermediate to EquiS and Eser (Fig. S5 in the Supporting Information).

Species divergence, hybridization, and demographic history

In the results of IMa2 analysis, the two species diverged around 1.78 Mya [95% confidence intervals (CI): 1.55–2.02 Mya]. The effective population size of *E. quinqueflorus* (8.13×10^6 , 95% CI: 7.12 – 9.14×10^6) was larger than that of *E. serrulatus* (3.46×10^6 , 95% CI: 2.94 – 4.02×10^6). The results showed

some evidence of gene flow between the two species. The estimate for the migration rate from *E. quinqueflorus* to *E. serrulatus* was 0.138, higher than the reverse direction (0.092) (Table 1 and Fig. 3A).

To further examine the divergence and hybridization among the three lineages (EquiN, EquiS, and Eser) according to the results of phylogenetic analyses and Bayesian clustering, we also carried out repeated runs of simulations with the DIYABC. The best-fit population model with ABC was scenario 3 (Fig. S6 in

the Supporting Information), which suggested that an initial split between Eser and EquiS at 0.93 Mya (95% CI: 0.27–1.81 Mya), then Eser and EquiS hybridized and produced EquiN at 0.22 Mya (95% CI: 0.08–0.40 Mya), each contributing 0.529 and 0.471 genetic ancestry (Table 2 and Fig. 3B). Our estimates of demographic parameters (Table 2 and Fig. S7 in the Supporting Information) using ABC were roughly consistent with the IM results. The EBSP simulations indicated the three lineages all experienced continuous recent population expansions (Fig. S8 in the Supporting Information).

Table 1. Parameters estimate and 95% CIs from IMa2 analyses.

Parameter	θ_A	θ_1	θ_2	t_1	N_A	N_1	N_2	T_1	$m_{1,2}$
MLE	1.430	7.568	17.789	0.975	6.54×10^5	3.46×10^6	8.13×10^6	1.78×10^6	0.092 (0.138)
HPD95Lo	0.431	6.433	15.59	0.848	1.97×10^5	2.94×10^6	7.12×10^6	1.55×10^6	0.034 (0.084)
HPD95Hi	3.347	8.792	20.00	1.107	1.53×10^6	4.02×10^6	9.14×10^6	2.02×10^6	0.168 (0.253)

θ_A and N_A , effective population size of ancestral population; θ_1 and N_1 , effective population size of *E. serrulatus*; θ_2 and N_2 , effective population size of *E. quinqueflorus*; t_1 and T_1 , divergence time of *E. quinqueflorus* and *E. serrulatus*; $m_{1,2}$, population migration rate from *E. serrulatus* to *E. quinqueflorus* (opposite direction in parentheses). θ and t are scaled by the mutation rate, while N and T are scaled by individuals or years.

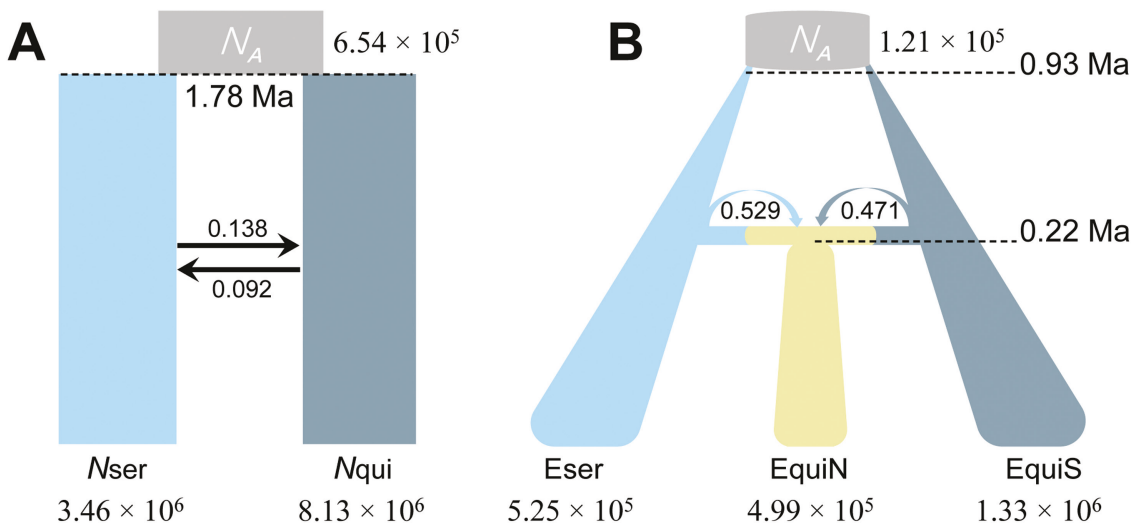


Figure 3. Demographic history of *E. quinqueflorus* and *E. serrulatus* inferred by IMa2 and DIYABC. A, Demographic model and coalescent simulation in IMa2. Dashed lines are time points at which populations split (1.78 Mya). The current population sizes of *E. serrulatus* and *E. quinqueflorus* are represented by N_{ser} (3.46×10^6 individuals) and N_{qui} (8.13×10^6 individuals), respectively, and the population size of their ancestor is denoted by N_A (6.54×10^5 individuals). Migration rates were shown on/under the solid arrows, and the arrow indicated the direction of migration. B, The most probable scenario (Scenario 3) with the ABC method implemented in DIYABC. Dashed lines are time points at which an initial split between Eser and EquiS (0.93 Mya), and Eser and EquiS hybridized and produced EquiN (0.22 Mya), with migration rate showed under the arrows. The population size of their ancestor is denoted by N_A (1.21×10^5 individuals), and the current population sizes of Eser, EquiN, and EquiS are illustrated.

Table 2. Demographic parameters estimate, and their 95% CIs, for scenario 3 that was best supported by the ABC model.

Parameter	N_A	N_1	N_2	N_3	T_0	T_1	r_a
Mean	1.21×10^5	5.25×10^5	1.33×10^6	4.99×10^5	0.93×10^6	0.22×10^6	0.529
Median	1.16×10^5	5.25×10^5	1.30×10^6	5.06×10^5	0.86×10^6	0.22×10^6	0.529
HPD95Lo	0.34×10^5	3.05×10^5	0.60×10^6	2.29×10^5	0.27×10^6	0.08×10^6	0.165
HPD95Hi	2.35×10^5	7.43×10^5	2.21×10^6	7.36×10^5	1.81×10^6	0.40×10^6	0.865

N_A , effective population size of ancestral population; N_1 , effective population size of Eser group; N_2 , effective population size of EquiS group; N_3 , effective population size of EquiN group; T_0 , divergence time of *E. quinqueflorus* and *E. serrulatus*; T_1 , divergence time of EquiN group; r_a , population migration rate between *E. quinqueflorus* and *E. serrulatus*. N are scaled by individuals, and T are scaled by years.

Ecological niche modelling and niche divergence

The AUC values of both species were > 0.9 , indicating their niche models had accurate discrimination. Based on the projected distributions, *E. quinqueflorus* has experienced range expansion since the LGM, and had the smallest distribution at LIG (Fig. 4A). The distribution of *E. serrulatus* was relatively stable during the late Quaternary. Distribution overlapping seems to be largest at the MH between the two species (Fig. 4A). The climatic niche overlap (identity test) showed that the

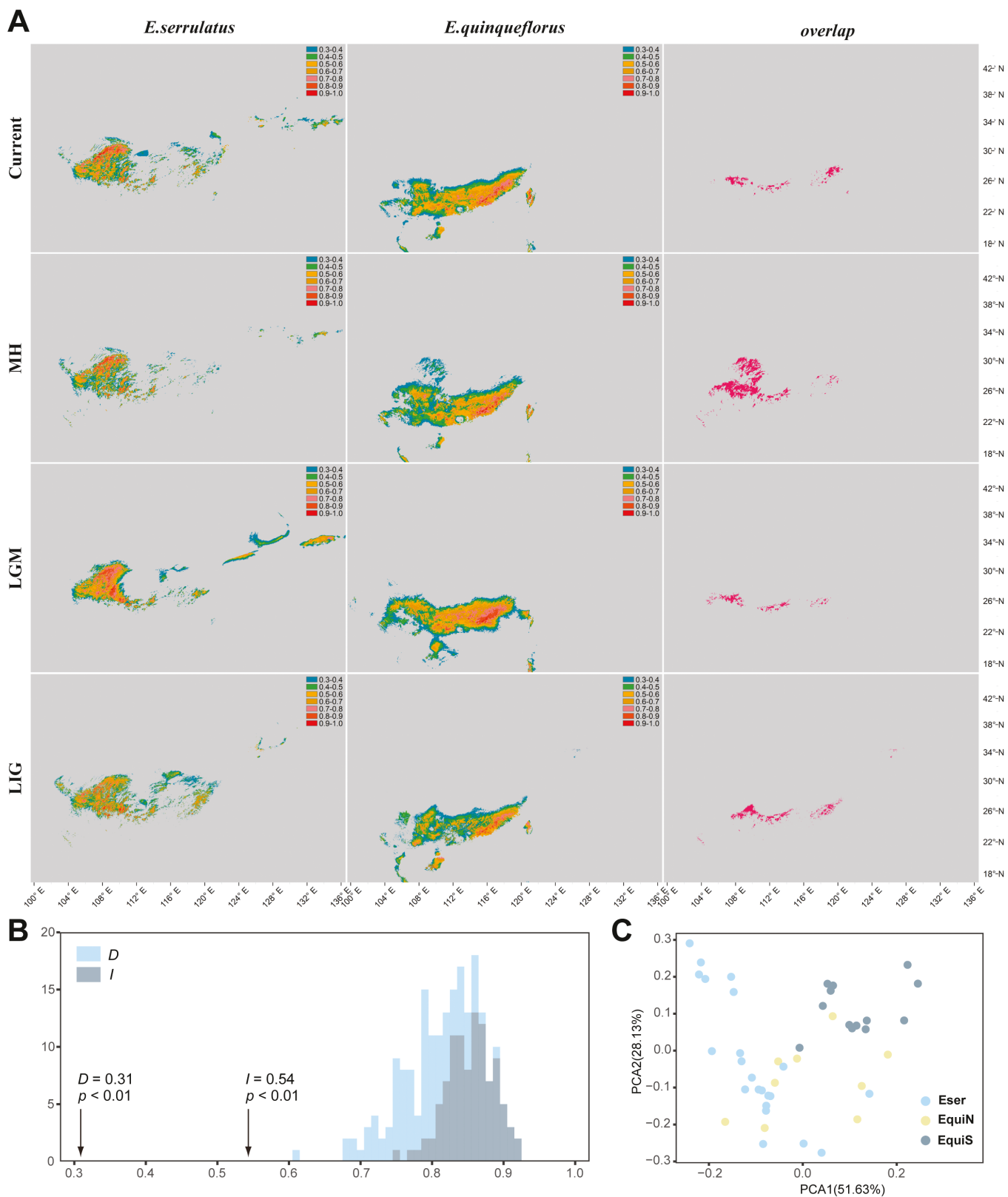


Figure 4. Ecological niche modelling and niche assessments of *E. quinqueflorus* and *E. serrulatus*. A, Potential distributions using MAXENT are shown during the present day (Current), the MH, the LGM, and the LIG climatic periods. Paleoclimate data of MH and LGM are under MIROC model. Overlap refers to the shared or intersecting area between the predicted distribution areas of two species. B, Climatic niche overlap (identity test) for *E. quinqueflorus* and *E. serrulatus*. Bars indicate the null distributions of *I* and *D*, and the arrow represents the actual values in MAXENT runs. C, PCA of climatic niche differences among genetically differentiated groups (Eser, EquiN, and EquiS) based on 19 climate variables.

observed values for I and D were significantly lower than those expected from pseudoreplicated data sets ($P < .01$) (Fig. 4B), indicating the two species were well differentiated ecologically. PCA analysis of climate variables also indicated an obvious divergence of the climatic envelope between *E. quinqueflorus* and *E. serrulatus*, with EquiN intermediate between them (Fig. 4C). The nonparametric Kruskal–Wallis multiple-range tests revealed that 14 out of the 19 bioclimatic variables showed significant differences between Eser and EquiS. Additionally, 10 of 19 bioclimatic variables showed significant differences between Eser and EquiN, while six of the 19 bioclimatic variables indicated significant differences between EquiS and EquiN (Fig. S9 in the Supporting Information).

DISCUSSION

Allopatric speciation across the Nanling Mountains

In this study, we found that *Enkianthus quinqueflorus* and *E. serrulatus* could be the products of allopatric speciation across the Nanling Mountains, as DIYABC revealed an initial period of allopatric divergence between Eser and EquiS and much later hybridization between them (Fig. 3). This result supports the conclusion that ecological speciation in the face of gene flow across ecotones, as well as the formation of primary hybrid zones (primary intergradation) along environmental gradients, is extremely rare (Abbott 2017). Ecotones commonly lie in areas of sharp climatic transition along environmental gradients, or zones of threshold or nonlinear responses to gradual gradients in the physical environment (Risser 1995, Kark 2007, 2012). Under such scenarios, ecological selection alone may promote the formation of new species, resulting in parapatric speciation across the ecotones (Smith *et al.* 1997, Schneider *et al.* 1999, Schilthuizen 2000, Nosil 2008). Although theoretical models have now demonstrated that ecological speciation with gene flow is feasible under particular conditions (Gavrilets 2004, Bolnick and Fitzpatrick 2007), speciation in the face of gene flow is generally thought to be difficult, because gene flow constrains population difference, thereby preventing the evolution of strong isolation (Coyne and Orr 2004, Nosil 2008). By far, only a few cases of plant ecological speciation with gene flow along an environmental gradient have been demonstrated (e.g. Andrew *et al.* 2013, Filatov *et al.* 2016).

Because most tropical plants cannot withstand environments below freezing temperature, there is a sharp decrease of tropical seed plants at the northern/southern boundaries of the tropical zone (Donoghue 2008), resulting in a transitional area (ecotone) from tropical zone to temperate zone (Zhu 2013, Ashton and Zhu 2020). This ecotone is prominent in east Asia (mainly in south and south-west China) because the tropical zone of Asia is broadly connected to subtropical or warm–temperate zones in China (Qian *et al.* 2017, Fan *et al.* 2022). During the middle and late Cenozoic towards the Quaternary, the global cooling and glacial climate (Zachos *et al.* 2001) have driven the tropical–subtropical ecotone shift towards the tropics (Qian *et al.* 2017), isolating many tropical plants into different northern refugia and possibly exposing some populations of tropical plants to cold climate (Fan *et al.* 2022). Under such scenarios, the populations in the northern refugia might have adapted to cold climate through

niche shifts (Donoghue 2008, Qian *et al.* 2017). This hypothesis has been illustrated by the population divergence history of *Machilus thunbergii* (Lauraceae) (Fan *et al.* 2022) and *Lindera aggregata* (Lauraceae) (Ye *et al.* 2019b). However, population differentiation does not necessarily proceed to speciation (Nosil 2012) and these studies did not provide solid evidence of niche evolution that is essential for adaptation to different temperature regimes across the freezing point (Donoghue 2008). By contrast, the different growth habits of *E. quinqueflorus* and *E. serrulatus* (evergreen versus deciduous) and their distinct ecological niches revealed in this study (Fig. 4B, C) clearly suggest that niche shift could have happened during the process of speciation. This study demonstrates that allopatric speciation and niche evolution across the tropical–subtropical ecotone in south China may be caused by range shifts and ecological adaptation that are associated with the Quaternary climate changes (Davis and Shaw 2001), supporting the dogma that allopatric ecological speciation is the easiest form of speciation (Nosil 2012), even along the latitudinal environmental gradients.

In this study, we found that *E. quinqueflorus* and *E. serrulatus* are the product of an allopatric speciation event that happened ~0.93 to 1.78 Mya (Tables 1, 2, Fig. 3), largely overlapped temporally with the mid-Pleistocene (MPT, 0.8–1.2 Mya). The MPT is characterized by a climate transition, an increase in the severity of glaciations, and the emergence of the ~100-ky glacial cycles (Clark *et al.* 2006). The earliest and largest glaciation in China (Wangkun glaciation, 700–500 kya) occurred shortly after the MPT (Cui *et al.* 2011). It is likely that the more severe glaciations during and after the MPT might have isolated some populations of the common ancestor of *E. quinqueflorus* and *E. serrulatus* to the north of the tropical–subtropical ecotone, enabling them to adapt to colder climate through niche evolution (Cavender-Bares *et al.* 2011, Fan *et al.* 2022). Our study further supports that the mid-Pleistocene is a critical period for population divergence and speciation of plant species in China during the Quaternary (e.g. Tian *et al.* 2015, Luo *et al.* 2016, Zhu *et al.* 2020, Fan *et al.* 2022).

Hybridization between *E. quinqueflorus* and *E. serrulatus* at the tropical–subtropical ecotone in south China

Cytonuclear discordance in phylogenies is a traditional signal of hybridization (Lee-Yaw *et al.* 2019). In this study, we found that individuals of populations 23–31 (EquiN, except for one individual in population 23) clustered with other individuals of *E. quinqueflorus* in the nuclear tree, but with those of *E. serrulatus* in the cpDNA tree (Fig. 2A, B, E, Supporting Information Fig. S4). In addition, ABC found that EquiN was derived from hybridization between EquiS and *E. serrulatus* (Eser) at 0.22 Mya (Fig. 3B), confirming that *E. quinqueflorus* and *E. serrulatus* may have hybridized and formed a hybrid zone mainly in the Nanling Mountains (Fig. 1).

In the results of STRUCTURE, however, EquiN individuals do not display a mixed ancestry of its putative parents *E. serrulatus* and EquiS when $K = 2$ as in most hybridization studies. To the contrary, EquiN shows its ancestry (coloured in yellow) and a greater or lesser proportion of EquiS ancestry when $K = 3$. Similar patterns have been observed in several hybridization studies (e.g. Elgvin *et al.* 2017, Ma *et al.* 2019). Ancient

hybridization and subsequent introgression (Ma *et al.* 2019), and limited resolution of our nuclear markers (Orozco-terWengel *et al.* 2011) could be responsible for the STRUCTURE pattern observed in this study. Anyway, the mixed ancestry of EquiN needs to be confirmed using high-throughput approaches such as whole-genome resequencing.

As noted before, *E. serotinus* highly resembles *E. quinqueflorus* morphologically. We attempted to identify *E. serotinus* according to collections from type localities. Five populations (23–27) that have a high yellow component correspond to *E. tubulatus* P. C. Tam, a species that was treated as a synonym of *E. serotinus* in Flora of China (Fang and Stevens 2005). Other populations of EquiN (28–32), however, are essentially *E. quinqueflorus*, their low proportion of yellow component might be caused by introgressive hybridization between *E. tubulatus* and *E. quinqueflorus*. Beyond our expectation, two populations of typical *E. serotinus* (populations 17 and 21, 17 is the type location of this species) belong to *E. serrulatus* genetically. They might be of hybrid origin like *E. tubulatus* and then backcrossed with *E. serrulatus*, however, their identity and origin need to be further verified.

Actually, the morphology of *E. tubulatus* is exactly intermediate to *E. quinqueflorus* and *E. serrulatus* (Fig. S5 in the Supporting Information), possessing leathery leaves such as *E. quinqueflorus*, but white flowers like *E. serrulatus*. This phenotypic intermediacy, coupled with phylogenetic discordance and the result of ABC modelling, clearly indicates that *E. tubulatus* could have originated from hybridization between *E. quinqueflorus* and *E. serrulatus*. In addition, our study implies that *E. tubulatus* might be a homoploid hybrid species through recombining phenotypes (flower colour and leaf texture in this case) to establish reproductive isolation between hybrid and parental lineages (Wang *et al.* 2021, Wu *et al.* 2023), because *E. tubulatus* constitutes a third cluster with its ancestry when $K = 3$ in STRUCTURE analysis. In the networks of individual nuclear locus and chloroplast DNA, *E. tubulatus* always possesses private haplotypes. This pattern is also observed in hybrid species that possess some degree of reproductive isolation from their parents (e.g. Ma *et al.* 2006, Gao *et al.* 2012, Guo *et al.* 2023). Of course, homoploid hybrid speciation is often considered extremely rare (Schumer *et al.* 2014), future works such as identifying the reassortment of parental barrier genes through comparative genomic analyses (e.g. Sun *et al.* 2020, Wang *et al.* 2021, Wu *et al.* 2023) are extremely needed to validate the hybrid species status of *E. tubulatus*.

The Nanling Mountains may be the tropical–subtropical transitional zone in terms of plant divergence and speciation

Freezing temperature is the principal restriction on the spreading out of the tropics for many tropical plant lineages, which can result in a sharp decrease in the tropical components at the north–south limit of the tropical zone (Donoghue 2008). In south and southwest China, Zhu and his colleagues found that 80% of tropical plant genera examined are confined to the south of the line at $\sim 22^{\circ} 30' \text{ N}$ (Zhu 2013, Ashton and Zhu 2020). They proposed that the line at $\sim 22^{\circ} 30' \text{ N}$ may represent the tropical–subtropical transitional zone in south and southwest China. By contrast, some tropical lineages can invade temperate climate regimes through niche evolution (Zanne *et al.* 2014), producing distinct populations or species to the north limit of the tropical zone.

This kind of ecophysiological line is more reasonable to represent the tropical–subtropical (warm–temperate) transitional zone and such a line can be illustrated using phylogeographic methods (Lin *et al.* 2018, Rana *et al.* 2023).

In this study, we found that a species pair of *Enkianthus* with contrasting growth habits (deciduous and evergreen) contacted secondarily and formed a hybrid zone around the Nanling Mountains, in line with several phylogeographic studies (Chen *et al.* 2012, Fan *et al.* 2016, Ye *et al.* 2019b, Fan *et al.* 2022). At a similar latitude in Central America, such an ecophysiological line has been reported in several phylogeographic and ecophysiological studies (e.g. Cavender-Bares 2007, Cavender-Bares *et al.* 2011). Although the ecophysiological performance of *E. quinqueflorus* and *E. serrulatus* under different temperatures remains to be determined and more empirical cases are needed, these results indicate that the Nanling Mountains may represent the tropical–subtropical transition zone of south China, at least from the perspective of the divergence and speciation of woody plants. Indeed, early in the 1960s, Zhu and Wan (1963) proposed that south of the Nanling Mountains is the tropical area in China, roughly south of 24° N – 25° N (Guangxi and Guangdong provinces) and up to 26° N in southeastern China (Fujian province) according to phenological observations. In addition, although the tropical areas in China in a narrow sense are limited to southern Hainan and the southern margin of Taiwan (Fang 2001, Fang *et al.* 2002) according to the Köppen–Geiger climate classification of the equatorial monsoon climate (Kottek *et al.* 2006), the newly published high-resolution bioclimate map of the world (Metzger *et al.* 2013) categorizes the whole south China (roughly south of the Nanling Mountains) into the hot and wet tropical zone, supporting that the Nanling Mountains may be an important biogeographical boundary that is critical for plant distribution and evolution. The Nanling Mountains have been renowned for its high conservation value as a biodiversity hotspot, an area of extensive human activities (Tang *et al.* 2006, Mi *et al.* 2021), and a dispersal corridor for plants and animals (Tian *et al.* 2015). This study suggests that the mountains may be a hotspot of speciation and hybridization for woody flowering plants, highlighting its high conservation value both as a museum and cradle of plant diversity (Lu *et al.* 2018).

SUPPLEMENTARY DATA

Supplementary data is available at *Botanical Journal of the Linnean Society* online.

ACKNOWLEDGEMENTS

This study was financially supported by the National Natural Science Foundation of China (nos 31660059, 31960049) and the Training Plan for Academic and Technical Leaders (leading talents) of major disciplines in Jiangxi, China (no. 20213BCJ22006).

DATA AVAILABILITY

The data underlying this article are available in the article and in its online supplementary material.

REFERENCES

Abbott RJ. Plant speciation across environmental gradients and the occurrence and nature of hybrid zones. *Journal of Systematics and Evolution* 2017;55:238–58. <https://doi.org/10.1111/jse.12267>

Anderberg AA. Cladistic interrelationships and major clades of the Ericales. *Plant Systematics and Evolution* 1993;184:207–31. <https://doi.org/10.1007/bf00937436>

Andrew RL, Kane NC, Baute GJ et al. Recent nonhybrid origin of sunflower ecotypes in a novel habitat. *Molecular Ecology* 2013;22:799–813. <https://doi.org/10.1111/mec.12038>

Ashton P, Zhu H. The tropical-subtropical evergreen forest transition in East Asia: An exploration. *Plant Diversity* 2020;42:255–80. <https://doi.org/10.1016/j.pld.2020.04.001>

Barton N, Gale KS. Genetic analysis of hybrid zones. In: Harrison RG (ed.), *Hybrid Zones and the Evolutionary Process*. New York: Oxford University Press, 1993, 13–45.

Barton NH, Hewitt GM. Analysis of hybrid zones. *Annual Review of Ecology, Evolution, and Systematics* 1985;16:113–48. <https://doi.org/10.1146/annurev.16.110185.000553>

Bolnick D, Fitzpatrick B. Sympatric speciation: models and empirical evidence. *Annual Review of Ecology, Evolution, and Systematics* 2007;38:459–87. <https://doi.org/10.1146/annurev.ecolsys.38.091206.095804>

Cavender-Bares J. Chilling and freezing stress in live oaks (*Quercus* section *Virentes*): intra- and inter-specific variation in PS II sensitivity corresponds to latitude of origin. *Photosynthesis Research* 2007;94:437–53. <https://doi.org/10.1007/s11120-007-9215-8>

Cavender-Bares J, Gonzalez-Rodriguez A, Pahlich A et al. Phylogeography and climatic niche evolution in live oaks (*Quercus* series *Virentes*) from the tropics to the temperate zone. *Journal of Biogeography* 2011;38:962–81. <https://doi.org/10.1111/j.1365-2699.2010.02451.x>

Chen Y, Compton SG, Liu M et al. Fig trees at the northern limit of their range: the distributions of cryptic pollinators indicate multiple glacial refugia. *Molecular Ecology* 2012;21:1687–701. <https://doi.org/10.1111/j.1365-294X.2012.05491.x>

Chen S, Milne R, Zhou R et al. When tropical and subtropical congeners met: Multiple ancient hybridization events within Eriobotrya in the Yunnan-Guizhou Plateau, a tropical-subtropical transition area in China. *Molecular Ecology* 2022;31:1543–61. <https://doi.org/10.1111/mec.16325>

Clark PU, Archer D, Pollard D et al. The middle Pleistocene transition: characteristics, mechanisms, and implications for long-term changes in atmospheric pCO₂. *Quaternary Science Reviews* 2006;25:3150–84. <https://doi.org/10.1016/j.quascirev.2006.07.008>

Cornuet JM, Pudlo P, Veyssié J et al. DIYABC v2.0: a software to make approximate Bayesian computation inferences about population history using single nucleotide polymorphism, DNA sequence and microsatellite data. *Bioinformatics* 2014;30:1187–9. <https://doi.org/10.1093/bioinformatics/btt763>

Coyne JA, Orr HA. *Speciation*. Sunderland: Sinauer Associates, Inc., 2004.

Cui ZJ, Chen YX, Zhang W et al. Research history, glacial chronology and origins of quaternary glaciations in China. *Quaternary Sciences* 2011;31:749–64. (in Chinese).

Darriba D, Taboada GL, Doallo R et al. jModelTest 2: more models, new heuristics and parallel computing. *Nature Methods* 2012;9:772. <https://doi.org/10.1038/nmeth.2109>

Davis MB, Shaw RG. Range shifts and adaptive responses to Quaternary climate change. *Science* 2001;292:673–9. <https://doi.org/10.1126/science.292.5517.673>

DeRaad DA, Applewhite EE, Tsai WLE et al. Hybrid zone or hybrid lineage: a genomic reevaluation of Sibley's classic species conundrum in *Pipilo* towhees. *Evolution; International Journal of Organic Evolution* 2023;77:852–69. <https://doi.org/10.1093/evolut/qpac068>

Donoghue MJA. phylogenetic perspective on the distribution of plant diversity. *Proceedings of the National Academy of Sciences of the United States of America* 2008;105:11549–55. <https://doi.org/10.1073/pnas.0801962105>

Doyle JJT, Doyle JL. Isolation of plant DNA from fresh tissue. *Focus* 1990;12:13–5.

Earl DA, vonHoldt BM. STRUCTURE HARVESTER: a website and program for visualizing STRUCTURE output and implementing the Evanno method. *Conservation Genetics Resources* 2012;4:359–61. <https://doi.org/10.1007/s12686-011-9548-7>

Elgyvin TO, Trier CN, Torresen OK et al. The genomic mosaicism of hybrid speciation. *Science Advances* 2017;3:e1602996. <https://doi.org/10.1126/sciadv.1602996>

Evanno G, Regnaut S, Goudet J. Detecting the number of clusters of individuals using the software STRUCTURE: a simulation study. *Molecular Ecology* 2005;14:2611–20. <https://doi.org/10.1111/j.1365-294X.2005.02553.x>

Excoffier L, Laval G, Schneider S. Arlequin (version 3.0): an integrated software package for population genetics data analysis. *Evolutionary Bioinformatics Online* 2007;1:47–50.

Fan D, Hu W, Li B et al. Idiosyncratic responses of evergreen broad-leaved forest constituents in China to the late Quaternary climate changes. *Scientific Reports* 2016;6:31044. <https://doi.org/10.1038/srep31044>

Fan D, Lei S, Liang H et al. More opportunities more species: Pleistocene differentiation and northward expansion of an evergreen broad-leaved tree species *Machilus thunbergii* (Lauraceae) in Southeast China. *BMC Plant Biology* 2022;22:35. <https://doi.org/10.1186/s12870-021-03420-9>

Fang JY. Re-discussion about the forest vegetation zonation in eastern China. *Acta Botanica Sinica* 2001;43:522–33. (in Chinese).

Fang JY, Song YC, Liu HY et al. Vegetation-climate relationship and its application in the division of vegetation zone in China. *Acta Botanica Sinica* 2002;44:1105–22. (in Chinese).

Fang RZ, Stevens PF, Enkianthus Lour. In: Wu ZT, Raven PH (eds), *Flora of China, Vol. 14*. Beijing: Science Press/St. Louis: Missouri Botanical Garden Press, 2005, 243–45.

Filatov DA, Osborne OG, Papadopoulos AST. Demographic history of speciation in a *Senecio* altitudinal hybrid zone on Mt. Etna. *Molecular Ecology* 2016;25:2467–81. <https://doi.org/10.1111/mec.13618>

Fu YX, Li WH. Statistical tests of neutrality of mutations. *Genetics* 1993;133:693–709. <https://doi.org/10.1093/genetics/133.3.693>

Gao J, Wang B, Mao JF et al. Demography and speciation history of the homoploid hybrid pine *Pinus densata* on the Tibetan Plateau. *Molecular Ecology* 2012;21:4811–27. <https://doi.org/10.1111/j.1365-294X.2012.05712.x>

Gavrilets S. *Fitness Landscapes and the Origin of Species* (MPB-41). Princeton: Princeton University Press, 2004.

Geng YY. Seed propagation of the evergreen Rhododendrons. In Chen YY (ed.), *Proceedings of the Fourth National Symposium on Biodiversity Conservation and Sustainable Use*. Hubei: Organized by the Biodiversity Committee of the Chinese Academy of Sciences, 2000, 126–34. (in Chinese).

Gompert Z, Mandeville EG, Buerkle CA. Analysis of population genomic data from hybrid zones. *Annual Review of Ecology, Evolution, and Systematics* 2017;48:207–29. <https://doi.org/10.1146/annurev-ecolsys-110316-022652>

Guo JF, Zhao W, Andersson B et al. Genomic clines across the species boundary between a hybrid pine and its progenitor in the eastern Tibetan Plateau. *Plant Communications* 2023;4:100574. <https://doi.org/10.1016/j.xplc.2023.100574>

Hall TA. BioEdit: A user-friendly biological sequence alignment editor and analysis program for Windows 95/98/NT. *Nucleic Acids Symposium Series* 1999;41:95–8. <https://doi.org/10.1021/bk-1999-0734.ch008>

Harrison RG. *Hybrid Zones and the Evolutionary Process*. Oxford: Oxford University Press, 1993.

Heled J, Drummond AJ. Bayesian inference of population size history from multiple loci. *BMC Evolutionary Biology* 2008;8:289. <https://doi.org/10.1186/1471-2148-8-289>

Hewitt GM. Hybrid zones-natural laboratories for evolutionary studies. *Trends in Ecology and Evolution* 1988;3:158–67. [https://doi.org/10.1016/0169-5347\(88\)90033-X](https://doi.org/10.1016/0169-5347(88)90033-X)

Hey J. Isolation with migration models for more than two populations. *Molecular Biology and Evolution* 2010;27:905–20. <https://doi.org/10.1093/molbev/msp296>

Hey J, Nielsen R. Multilocus methods for estimating population sizes, migration rates and divergence time, with applications to the divergence of *Drosophila pseudoobscura* and *D. persimilis*. *Genetics* 2004; **167**:747–60. <https://doi.org/10.1534/genetics.103.024182>

Hey J, Nielsen R. Integration within the Felsenstein equation for improved Markov chain Monte Carlo methods in population genetics. *Proceedings of the National Academy of Sciences of the United States of America* 2007; **104**:2785–90. <https://doi.org/10.1073/pnas.0611164104>

Hubisz MJ, Falush D, Stephens M et al. Inferring weak population structure with the assistance of sample group information. *Molecular Ecology Resources* 2009; **9**:1322–32. <https://doi.org/10.1111/j.1755-0998.2009.02591.x>

Kark S. Effects of ecotones on biodiversity. In: Levin SA (ed.), *Encyclopedia of Biodiversity*. London: Academic Press/Elsevier, 2007, 142–8. <https://doi.org/10.1016/B978-012226865-6/00573-0>

Kark S. Ecotones and ecological gradients. In: Meyers RA (ed.), *Encyclopedia of Sustainability Science and Technology*. New York: Springer Science and Business Media, 2012, 147–60.

Kottel M, Grieser J, Beck C et al. World map of the Köppen-Geiger climate classification updated. *Meteorologische Zeitschrift* 2006; **15**:259–63. <https://doi.org/10.1127/0941-2948/2006/0130>

Kou Y, Liao Y, Toivainen T et al. Evolutionary genomics of structural variation in Asian Rice (*Oryza sativa*) domestication. *Molecular Biology and Evolution* 2020; **37**:3507–24. <https://doi.org/10.1093/molbev/msaa185>

Kumar S, Stecher G, Tamura K. MEGA7: molecular evolutionary genetics analysis version 7.0 for bigger datasets. *Molecular Biology and Evolution* 2016; **33**:1870–4. <https://doi.org/10.1093/molbev/msw054>

Lee-Yaw JA, Grassa CJ, Joly S et al. An evaluation of alternative explanations for widespread cytonuclear discordance in annual sunflowers (*Helianthus*). *The New Phytologist* 2019; **221**:515–26. <https://doi.org/10.1111/nph.15386>

Leigh J, Bryant D. PopART: full-feature software for haplotype network construction. *Methods in Ecology and Evolution* 2015; **6**:1110–6. <https://doi.org/10.1111/2041-210X.12410>

Liang H, Jiang L, Li D et al. A new synonym of *Enkianthus perulatus* (Ericaceae) in East Asia, based on morphological and molecular evidence. *PhytoKeys* 2022; **214**:61–74. <https://doi.org/10.3897/phytokeys.214.94294>

Librado P, Rozas J. DnaSP v5: a software for comprehensive analysis of DNA polymorphism data. *Bioinformatics* 2009; **25**:1451–2. <https://doi.org/10.1093/bioinformatics/btp187>

Lin N, Deng T, Moore MJ et al. Phylogeography of *Parasyncalathium soulieii* (Asteraceae) and its potential application in delimiting phylogeoregions in the Qinghai-Tibet Plateau (QTP)-Hengduan Mountains (HDM) hotspot. *Frontiers in Genetics* 2018; **9**:171. <https://doi.org/10.3389/fgene.2018.00171>

Lu LM, Mao LF, Yang T et al. Evolutionary history of the angiosperm flora of China. *Nature* 2018; **554**:234–8. <https://doi.org/10.1038/nature25485>

Luo D, Yue JP, Sun WG et al. Evolutionary history of the subnival flora of the Himalaya-Hengduan Mountains: first insights from comparative phylogeography of four perennial herbs. *Journal of Biogeography* 2016; **43**:31–43. <https://doi.org/10.1111/jbi.12610>

Ma XF, Szmidt AE, Wang XR. Genetic structure and evolutionary history of a diploid hybrid pine *Pinus densata* inferred from the nucleotide variation at seven gene loci. *Molecular Biology and Evolution* 2006; **23**:807–16. <https://doi.org/10.1093/molbev/msj100>

Ma Y, Wang J, Hu Q et al. Ancient introgression drives adaptation to cooler and drier mountain habitats in a cypress species complex. *Communications Biology* 2019; **2**:213. <https://doi.org/10.1038/s42003-019-0445-z>

Mayr E. Isolation as an evolutionary factor. *Proceedings of the American Philosophical Society* 1959; **103**:221–30.

Metzger MJ, Bunce RGH, Jongman RHG et al. A high-resolution bioclimate map of the world: a unifying framework for global biodiversity research and monitoring. *Global Ecology and Biogeography* 2013; **22**:630–8. <http://doi.org/10.1111/geb.12022>

Mi X, Feng G, Hu Y et al. The global significance of biodiversity science in China: an overview. *National Science Review* 2021; **8**:nwab032. <https://doi.org/10.1093/nsr/nwab032>

Moore WS, Price JT. Nature of selection in the northern flicker hybrid zone and its implications for speciation theory. In: Harrison RG (ed.), *Hybrid Zones and the Evolutionary Process*. New York: Oxford University Press, 1993, 196–225.

Nosil P. Speciation with gene flow could be common. *Molecular Ecology* 2008; **17**:2103–6. <https://doi.org/10.1111/j.1365-294X.2008.03715.x>

Nosil P. *Ecological Speciation*. Oxford: Oxford University Press, 2012.

Orozco-terWengel P, Corander J, Schlötterer C. Genealogical lineage sorting leads to significant, but incorrect Bayesian multilocus inference of population structure. *Molecular Ecology* 2011; **20**:1108–21. <https://doi.org/10.1111/j.1365-294X.2010.04990.x>

Pereira RJ, Sasaki MC, Burton RS. Adaptation to a latitudinal thermal gradient within a widespread copepod species: the contributions of genetic divergence and phenotypic plasticity. *Proceedings Biological Sciences* 2017; **284**:20170236. <https://doi.org/10.1098/rspb.2017.0236>

Phillips S, Dudík M. Modeling of species distributions with MAXENT: new extensions and a comprehensive evaluation. *Ecography* 2008; **31**:161–75. <https://doi.org/10.1111/j.0906-7590.2008.5203.x>

Price MN, Dehal PS, Arkin AP. FastTree: computing large minimum evolution trees with profiles instead of a distance matrix. *Molecular Biology and Evolution* 2009; **26**:1641–50. <https://doi.org/10.1093/molbev/msp077>

Pritchard JK, Stephens M, Donnelly P. Inference of population structure using multilocus genotype data. *Genetics* 2000; **155**:945–59. <https://doi.org/10.1093/genetics/155.2.945>

Qian H, Jin Y, Ricklefs RE. Phylogenetic diversity anomaly in angiosperms between eastern Asia and eastern North America. *Proceedings of the National Academy of Sciences of the United States of America* 2017; **114**:11452–7. <https://doi.org/10.1073/pnas.1703985114>

Rambaut A, Drummond AJ, Xie D et al. Posterior summarization in Bayesian phylogenetics using Tracer 1.7. *Systematic Biology* 2018; **67**:901–4. <https://doi.org/10.1093/sysbio/syy032>

Rana HK, Rana SK, Luo D et al. Existence of biogeographic barriers for the long-term Neogene–Quaternary divergence and differentiation of *Koenigia forrestii* in the Himalaya–Hengduan Mountains. *Botanical Journal of the Linnean Society* 2023; **201**:230–53. <https://doi.org/10.1093/botlinnean/boc045>

Rieseberg LH, Archer MA, Wayne RK. Transgressive segregation, adaptation and speciation. *Heredity* 1999; **83** (Pt 4):363–72. <https://doi.org/10.1038/sj.hdy.6886170>

Risser PG. The status of the science examining ecotones. *BioScience* 1995; **45**:318–25. <https://doi.org/10.2307/1312492>

Sakai A, Larcher W. *Frost Survival of Plants: Responses and Adaptation to Freezing Stress*. Berlin: Springer-Verlag, 1987.

Schilthuizen ME. Speciation-prone. *Trends in Ecology and Evolution* 2000; **15**:130–1. [https://doi.org/10.1016/s0169-5347\(00\)01839-5](https://doi.org/10.1016/s0169-5347(00)01839-5)

Schneider CJ, Smith TB, Larison B et al. A test of alternative models of diversification in tropical rainforests: ecological gradients vs. rainforest refugia. *Proceedings of the National Academy of Sciences of the United States of America* 1999; **96**:13869–73. <https://doi.org/10.1073/pnas.96.24.13869>

Schumer M, Rosenthal GG, Andolfatto P. How common is homoploid hybrid speciation? *Evolution* 2014; **68**:1553–60. <https://doi.org/10.1111/evo.12399>

Smith T, Wayne R, Girman D et al. A role for ecotones in generating rainforest biodiversity. *Science* 1997; **276**:1855–7. <https://doi.org/10.1126/science.276.5320.1855>

Stacklies W, Redestig H, Scholz M et al. pcaMethods—a bioconductor package providing PCA methods for incomplete data. *Bioinformatics* 2007; **23**:1164–7. <https://doi.org/10.1093/bioinformatics/btm069>

Stankowski S, Shipilina D, Westram AM. Hybrid zones. *The Encyclopedia of Life Sciences* 2021; **2**:1–12. <https://doi.org/10.1002/9780470015902.a0029355>

Sun Y, Lu Z, Zhu X et al. Genomic basis of homoploid hybrid speciation within chestnut trees. *Nature Communications* 2020; **11**:3375. <https://doi.org/10.1038/s41467-020-17111-w>

Tang Z, Wang Z, Zheng C *et al.* Biodiversity in China's mountains. *Frontiers in Ecology and the Environment* 2006;4:347–52. [https://doi.org/10.1890/1540-9295\(2006\)004\[0347:bicm\]2.0.co;2](https://doi.org/10.1890/1540-9295(2006)004[0347:bicm]2.0.co;2)

Tian S, Lei SQ, Hu W *et al.* Repeated range expansions and inter-/post-glacial recolonization routes of *Sargentodoxa cuneata* (Oliv.) Rehd. et Wils. (Lardizabalaceae) in subtropical China revealed by chloroplast phylogeography. *Molecular Phylogenetics and Evolution* 2015;85:238–46. <https://doi.org/10.1016/j.ympev.2015.02.016>

Tsutsumi C, Hirayama Y. The phylogeny of Japanese Enkianthus species (Ericaceae). *Bulletin of the National Museum of Nature and Science* 2012;38:11–7.

Wang XR, Szmidt AE. Evolutionary analysis of *Pinus densata* (Masters), a putative Tertiary hybrid. *TAG. Theoretical and Applied Genetics. Theoretische und angewandte Genetik* 1990;80:641635–7640. <https://doi.org/10.1007/BF00224224>

Wang Z, Jiang Y, Bi H *et al.* Hybrid speciation via inheritance of alternate alleles of parental isolating genes. *Molecular Plant* 2021;14:208–22. <https://doi.org/10.1016/j.molp.2020.11.008>

Warren DL, Glor RE, Turelli M. Environmental niche equivalency versus conservatism: quantitative approaches to niche evolution. *Evolution* 2008;62:2868–83. <https://doi.org/10.1111/j.1558-5646.2008.00482.x>

Warren D, Glor R, Turelli M. ENMTools: a toolbox for comparative studies of environmental niche models. *Ecography* 2010;33:607–11. <https://doi.org/10.1111/j.1600-0587.2009.06142.x>

Watterson GA. On the number of segregating sites in genetical models without recombination. *Theoretical Population Biology* 1975;7:256–76. [https://doi.org/10.1016/0040-5809\(75\)90020-9](https://doi.org/10.1016/0040-5809(75)90020-9)

Wielstra B. Hybrid zones. *Current Biology* 2021;31:R108–9. <https://doi.org/10.1016/j.cub.2020.11.046>

Wright S. The genetical structure of populations. *Annals of Eugenics* 1951;15:323–54. <https://doi.org/10.1111/j.1469-1809.1949.tb02451.x>

Wu H, Wang Z, Zhang Y *et al.* Hybrid origin of a primate, the gray snub-nosed monkey. *Science* 2023;380:eabl4997. <https://doi.org/10.1126/science.abl4997>

Ye J, Lu L, Liu B *et al.* Phylogenetic delineation of regional biota: a case study of the Chinese flora. *Molecular Phylogenetics and Evolution* 2019a;135:222–9. <https://doi.org/10.1016/j.ympev.2019.03.011>

Ye JW, Li DZ, Hampe A. Differential Quaternary dynamics of evergreen broadleaved forests in subtropical China revealed by phylogeography of *Lindera aggregata* (Lauraceae). *Journal of Biogeography* 2019b;46:1112–23. <https://doi.org/10.1111/jbi.13547>

Yoichi W, Tamaki I, Sakaguchi S *et al.* Population demographic history of a temperate shrub, *Rhododendron weyrichii* (Ericaceae), on continental islands of Japan and South Korea. *Ecology and Evolution* 2016;6:8800–10. <https://doi.org/10.1002/ece3.2576>

Zachos J, Pagani M, Sloan L *et al.* Trends, rhythms, and aberrations in global climate 65 Ma to present. *Science* 2001;292:686–93. <https://doi.org/10.1126/science.1059412>

Zanne AE, Tank DC, Cornwell WK *et al.* Three keys to the radiation of angiosperms into freezing environments. *Nature* 2014;506:89–92. <https://doi.org/10.1038/nature12872>

Zhou R, Ci X, Hu J *et al.* Transitional areas of vegetation as biodiversity hotspots evidenced by multifaceted biodiversity analysis of a dominant group in Chinese evergreen broad-leaved forests. *Ecological Indicators* 2023;147:110001. <https://doi.org/10.1016/j.ecolind.2023.110001>

Zhu H. Geographical elements of seed plants suggest the boundary of the tropical zone in China. *Palaeogeography, Palaeoclimatology, Palaeoecology* 2013;386:16–22. <https://doi.org/10.1016/j.palaeo.2013.04.007>

Zhu KZ, Wan MW. *Phenology* (in Chinese). Beijing: Scientific Education Press, 1963.

Zhu SS, Comes HP, Tamaki I *et al.* Patterns of genotype variation and demographic history in *Lindera glauca* (Lauraceae), an apomict-containing dioecious forest tree. *Journal of Biogeography* 2020;47:2002–16. <https://doi.org/10.1111/jbi.13874>

Zou J, Sun Y, Li L *et al.* Population genetic evidence for speciation pattern and gene flow between *Picea wilsonii*, *P. morrisonicola* and *P. neoveitchii*. *Annals of Botany* 2013;112:1829–44. <https://doi.org/10.1093/aob/mct241>